UNITED NATIONS UNIVERSITY

GEOTHERMAL TRAINING PROGRAMME
Orkustofnun, Grensasvegur 9,
IS-108 Reykjavik, Iceland

Reports 2010
Number 23

NOISE ASSESSMENT AND H_2S DISPERSION AT OLKARIA GEOTHERMAL POWER PLANT, KENYA

Cornelius J. Ndetei
Kenya Electricity Generating Company Ltd. – KenGen
Olkaria Geothermal Project
P.O. Box 785, 20117 Naivasha
KENYA
cndetei@gmail.com, cndetei@kengen.co.ke,

ABSTRACT

The goal of this study was to characterise noise levels and hydrogen sulphide (H_2S) dispersion at Olkaria geothermal power stations in Kenya. Noise levels due to the exploitation of geothermal resources at Olkaria were assessed both in space and time, and the measured levels were compared with the standard limits set by the Kenyan National Environment Agency and the World Health Organisation. H_2S dispersion at Olkaria was modelled and predicted using AERMOD, which is a steady-state Gaussian model. Two modelling scenarios were assessed, scenario one considered H_2S emissions from the existing Olkaria I and Olkaria II power stations, whereas scenario two considered predicted concentrations in light of the addition of Olkaria IV to the existing power stations. One, eight and twenty-four hour averaging periods were selected for the study. Modelling results showed that no significant health and environmental impacts were expected outside the power-plant boundaries due to the existing or proposed power plants. However, it was found likely that odours would be detectable over a wide area. In general, averaged gas concentrations were high close to the emission sources and rapidly diluted depending on weather conditions. The behaviour of the plume was also considered; it was noted that gas emissions through cooling tower plumes achieved better plume rise than gas discharged through gas ejectors.

1. INTRODUCTION

In comparison to fossil and nuclear power sources, geothermal resources are a clean, reliable and abundant source of energy, with great potential to meet an increasing share of the world´s expanding energy needs (Rybach, 2003). Due to burgeoning populations and escalating economies, geothermal energy is inexorably gaining momentum in the many parts of the world endowed with the resource. It is now being utilised in 78 countries worldwide for both direct and indirect uses (Lund et al., 2010).

Kenya is the first country in Sub-Saharan Africa to tap power from the Earth's crust in a significant fashion (Karekezi and Kithyoma, 2003). The country has plentiful geothermal resources that have not been exploited to their full potential. The resources are located in the Kenyan Rift (Figure 1), and recent studies of geothermal explorations revealed that the geothermal potential in the rift exceeds 7,000 megawatts of electricity (MWe) (Simiyu, 2008). This could meet all of Kenya's electricity needs over the next 20 years (Simiyu, 2010), with a power-demand growth estimated at 8% annually.

The Least Cost Power Development Plan (2010-2030) prepared by the Government of Kenya, indicates that geothermal plants have the lowest unit cost and, therefore, are suitable for base load and, as such, are recommended for additional expansion (Republic of Kenya, 2010). Geothermal energy in Kenya is primarily utilised for electricity production, currently 202 MWe. Direct uses of geothermal energy in the country include greenhouses, drying agricultural products, swimming, therapeutic bathing, and aquaculture. About 14 geothermal sites have been identified in the Kenyan Rift (Figure 1). These prospect fields from south to north are Lake Magadi, Suswa, Longonot, Olkaria, Eburru, Badlands, Menengai, Arus Bogoria, Lake Baringo, Korosi, Paka, Silali, Emuruangogolak, Namarunu and Barrier Volcano. Only the Olkaria geothermal field has been developed. The other fields are at various reconnaissance and surface exploration stages, except for Eburru where exploration drilling has been undertaken.

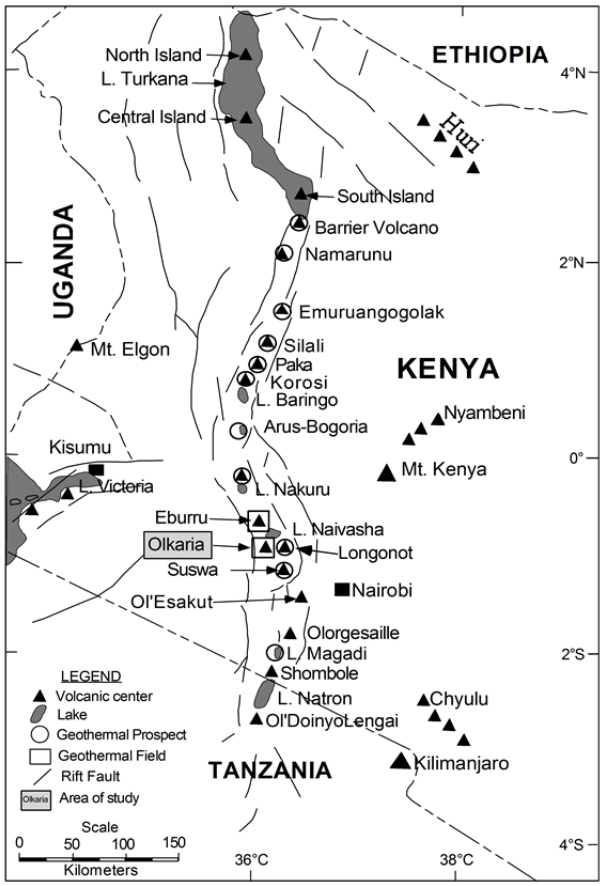

FIGURE 1: Kenya geothermal fields and prospects (Lagat, 2004)

The main environmental concerns arising from geothermal operations are associated with noise and the discharge of non-condensable gases such as hydrogen sulphide (H_2S), carbon dioxide (CO_2) and methane (CH_4) into the atmosphere. Geothermal fluids also contain small proportions of ammonia, mercury, radon and boron (Komurcu and Akpinar, 2009). CO_2, which is usually the major constituent of the gas present in geothermal fluids, and CH_4, a minor constituent, both require attention because of their roles as greenhouse gases (Giroud and Arnórsson, 2005). Among all non-condensable gases emitted due to geothermal exploitation, H_2S has the greatest environmental concern not only because of its noxious smell in low concentrations but also due to its toxicity and health impacts at high concentrations, and its tendency to concentrate in hollows and low-lying areas due to its high density (Kristmannsdóttir et al., 2000). Some projects have been objected to by nearby populations due to the discharge of H_2S in high concentrations, such as in Puna in Hawaii (Anderson, 1991), or were prevented, as at Milos in Greece (Marouli and Kaldellis, 2001). As a way of determining environmental impacts associated with noise and hydrogen sulphide, various modelling techniques have been employed in distinct parts of the world such as in Mexico (Gallegos-Ortega et al., 2000) and Iceland (Nyagah, 2006) among others. This study focuses on assessing noise and H_2S dispersion at the existing Olkaria I and Olkaria II power plants and the proposed Olkaria IV power plant in Kenya.

2. AIMS AND OBJECTIVES

The goal of this study is to assess noise levels and hydrogen sulphide concentrations at Olkaria geothermal field in Kenya, and to model hydrogen sulphide (H_2S) dispersion in the area. In order to accomplish this aim, the following specific objectives will be achieved:

- Assessment of the temporal and spatial distributions of near ground noise and H_2S due to exploitation of Olkaria I and Olkaria II power stations;

- Prediction of H_2S concentrations due to emissions from the existing Olkaria I and Olkaria II power stations and the proposed Olkaria IV power station, using a Gaussian dispersion model; and
- Assessment of any potential health and environmental impacts due to H_2S emissions from the power plants.

3. BACKGROUND

3.1 Environmental impacts and health implications of hydrogen sulphide

Hydrogen sulphide (H_2S) is produced naturally and as a result of human activity (WHO, 2003). Geothermal development is associated with emissions of hydrogen sulphide; the most important points of emission in plants are chimneys for venting non-condensable gases, cooling towers, silencers and traps in the vapour duct (Nyagah, 2006). Noise sources include the cooling towers and the plant housing the turbines. H_2S, as discussed in detail by WHO (2003), is a colourless, flammable gas, with a characteristic odour of rotten eggs at low concentrations, and it is toxic in high concentrations. It is rapidly oxidised in air and in solution and is corrosive to many metals; it may discolour paint by its reaction with the metals present in the pigments. Because of its high density and negative buoyancy, H_2S can accumulate in low-lying areas such as cellars and basements, and can be imperceptible at lethal concentrations (Hunt, 2001). The measurement units for H_2S in the air are parts per million (ppm) or milligrams per cubic metre (mg/m^3). At an air temperature of 20°C and 101.3 kPa, 1 ppm of H_2S is equivalent to 1.4 mg/m^3, hence 1mg/m^3 of the gas is equivalent to 0.71 ppm (WHO, 2003). This conversion was adopted in this report. The concentration of the gas in air in unpolluted areas is very low, between 0.03 and 0.1 $\mu g/m^3$.

According to WHO (1981), the toxic effects of H_2S vary according to the dosage and are classified in scientific literature into three categories, namely acute, sub-acute and chronic (for further details, see WHO (1981)). Chambers and Johnson (2009) reported that exposure to lower concentrations of hydrogen sulphide could result in eye irritation, sore throat, coughing, nausea, shortness of breath, and fluid in the lungs. However, long-term, low-level exposure could result in fatigue, loss of appetite, headaches, irritability, poor memory, and dizziness (Chambers and Johnson, 2009).

In humans, H_2S is unlikely to bio-concentrate because it is excreted through the urine, intestines and expired air (WHO, 2003). However, it can be a nuisance at very low concentrations of about 0.3 ppm. Table 1 summarises the human health effects of H_2S at various concentrations.

There are no ambient air quality standards for H_2S currently in force in Kenya. Hence, WHO guidelines and standards have been adopted in many studies in Kenya. According to WHO (2000) guidelines, 24-hour average concentrations should not be permitted to exceed 0.1 ppm beyond the immediate power station boundary. The National Institute for Occupational Safety and Health (NIOSH), and the American Conference of Governmental and Industrial Hygienists (ACGIH) air quality standards for the protection of occupational health give limits of 10 ppm for H_2S in atmospheric air (Webster, 1995). Thus, in workplaces, H_2S concentrations should not exceed 10 ppm over an 8 hour period for staff working five days a week.

3.2 Noise impacts on health and the associated environmental regulations in Kenya

Noise is associated with both auditory and non-auditory impacts. Exposure to noise levels of relatively high degrees can lead to direct hearing loss or hearing impairment (Ismail et al., 2009). The non-auditory impacts include annoyance and disruption of basic activities such as sleep, rest, communication, concentration, and might affect health and physiological well-being (WHO, 1999;

TABLE 1: Health impacts of H_2S at several key concentrations (Chambers and Johnson, 2009)

H_2S concent. (ppm)	**Effects on humans**
0.0047	Recognition threshold concentration at which 50% of most humans can detect the characteristic odour of hydrogen sulphide, normally described as resembling that of a rotten egg
10 – 20	Threshold for eye irritation
50 – 100	Eye damage
150 – 250	Olfactory nerve is paralysed after a few inhalations; sense of smell disappears, often together with awareness of danger
320 – 530	Leads to pulmonary oedema with the possibility of death
500	30 to 60 minute exposure can result in headache, dizziness, and staggering followed by unconsciousness and respiratory failure
530 – 1000	Causes strong stimulation of the central nervous system and rapid breathing leading to lack of breath
800	Lethal concentration for 50% of humans after 5 minutes exposure
>1000	Causes immediate collapse with loss of breathing (even following inhalation of a single breath of H_2S gas)

Muzet, 2007). Acute noise exposure has been shown to induce physiological responses such as increased blood pressure and heart rate (Haralabidis et al., 2008). Since acute exposure to noise has been linked to transient increases in blood pressure and levels of stress hormones in experimental settings, it has been hypothesized that long-term exposure to noise may have adverse effects on health (Babisch, 2000). Key environmental regulations concerned with regulating noise levels include the first and second Schedule of Environment Management and Co-ordination (noise and excessive vibration pollution) Regulations of 2009, as set up by the Kenyan National Environmental Management Authority (NEMA) (Republic of Kenya, 2009). According to the first schedule, noise levels should not exceed 35 dB(A) during the night (20:01 to 06:00 hours) in residential or commercial zones. Similarly, daytime levels (06:01 to 20:00 hours) should not exceed 45 dB(A) in indoor residential zones, 50 dB(A) in outdoor residential zones or 60 dB(A) in commercial zones. However, the second schedule requires that the maximum permissible noise levels for construction sites during night time (18:01 to 06:00 hours) should not exceed 35 dB(A) in residential zones or 65 dB(A) in commercial zones (Republic of Kenya, 2009). Noise levels during the day (06:01 to 18:00 hours) for construction sites should not exceed 60 dB(A) in residential zones or 75 dB(A) in commercial/industrial zones. Note that noise is measured in decibels (dB), and the measurements are averaged over a certain time period, hence the units are in dB(A). The World Bank finances most geothermal projects in developing countries, including Kenya. Consequently, such projects should comply with the World Bank and WHO guidelines. Table 2 summarises World Bank and WHO noise exposure limit standards at the workplace and in residential areas.

TABLE 2: World Bank and WHO noise exposure standards (World Bank, 1998; World Bank, 2007)

Receptor	**Maximum allowable L_{eq}^{*} (hourly) in dB(A)**			
	World Bank		**World Health Organization**	
	Day time (07:00-22:00 hrs)	**Night time (22:00-07:00 hrs)**	**Day time (07:00-22:00 hrs)**	**Night time (22:00-07:00 hrs)**
Residential, institutional and educational	55	45	50	45
Industrial and commercial	70	70	85	85

$^{*}L_{eq}$ is the equivalent continuous sound pressure level

3.3 Situation in Kenya

In Kenya, geothermal development has been successfully carried out in the Olkaria field. The field is located in the Naivasha district, which is among the densely populated districts of the country supporting 376,243 people, according to the 2009 population census (KNBS, 2009), and is 27 km south of Naivasha town. The Olkaria field, also referred as the Greater Olkaria geothermal area (GOGA), covers an area of approximately 80 km^2 (Simiyu, 2008). The Olkaria field has been demarcated into seven sub-fields, namely Olkaria East, Olkaria West, Olkaria Northwest, Olkaria Northeast, Olkaria Central, Olkaria Domes and Olkaria Southwest (Opondo, 2007), shown in Figure 2.

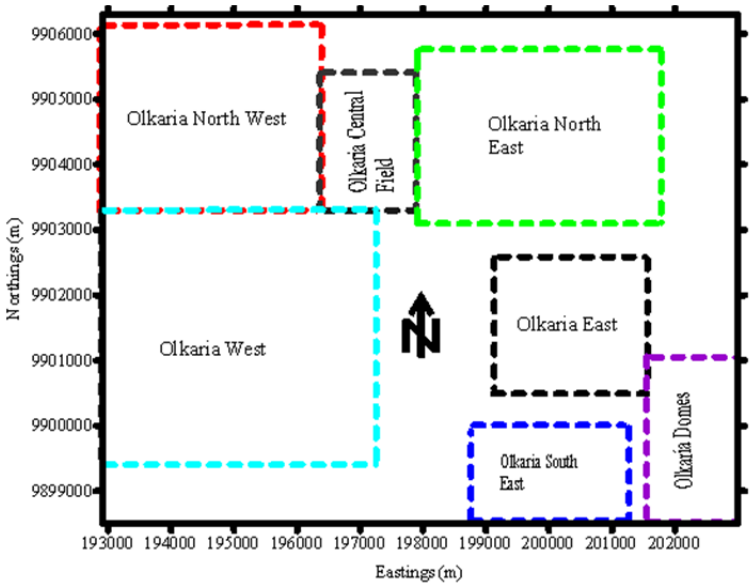

FIGURE 2: Location of the geothermal fields in the Greater Olkaria geothermal area (Opondo, 2007)

For ease of discussion, the Olkaria field has been broadly categorised into four sub-areas, namely Olkaria I, Olkaria II, Olkaria III and Olkaria IV. The resource from Olkaria field is being utilised mainly for electric power generation (202 MWe), but also for direct use (18 MWt) (Simiyu, 2010). The proven geothermal resource in the geothermal field is more than 450 MWe (Simiyu, 2010) and accelerated development is envisaged in the near future.

Olkaria I power plant is located in the East field and has three units, each generating 15 MWe, whereas Olkaria II power plant is located in the Northeast field and has three units, each generating 35 MWe. The three units in Olkaria I were commissioned in 1981, 1983 and 1985, respectively, while two of the units in Olkaria II were commissioned in 2003 (Simiyu, 2010), and the third unit was commissioned in May 2010. Both Olkaria I and II power plants are owned and operated by the Kenya Electricity Generating Company (KenGen), which is partly owned by the state (70%) and partly by the private sector (30%). The company is in the process of developing two 70 MWe units at Olkaria IV (Olkaria Domes) that are expected to be commissioned in 2012/2013 (Simiyu, 2010). Olkaria III power plant generates 48 MWe and is located in the West field; it is operated by Ormat, an independent power producer. Oserian Development Company, which specialises in flower farming for export purposes, generates 4 MWe for its internal uses.

Olkaria geothermal field is a sensitive area, and studies have been carried out to establish the effects of noise and air pollution arising from geothermal exploitation. Kollikho and Kubo (2001) conducted a study to investigate the effects of geothermal emissions from cooling towers and gas ejectors on flowers cultivated within the vicinity of Olkaria. Their results did not show any significant difference in the yield of flowers grown 600 and 1200 m away from the emission sources.

3.4 Proximity to residential areas

The existing Olkaria I and Olkaria II power plants are located inside Hell's Gate National Park, which is a protected area for wildlife conservation (Figure 3). Olkaria II power plant is located about 5 km south of Lake Naivasha, the only fresh water lake in the Kenyan Rift Valley. About 3 km northwest of the power station is the Oserian Development Company, which is a commercially vital floricultural

farm that grows high quality cut flowers for export to Europe. There are some residential areas and community settlements neighbouring Olkaria geothermal field, shown in Figure 3. The approximate distance between Olkaria I and Olkaria II power stations is 3.3 km, while the distance between Olkaria II and the site for Olkaria IV is about 7 km.

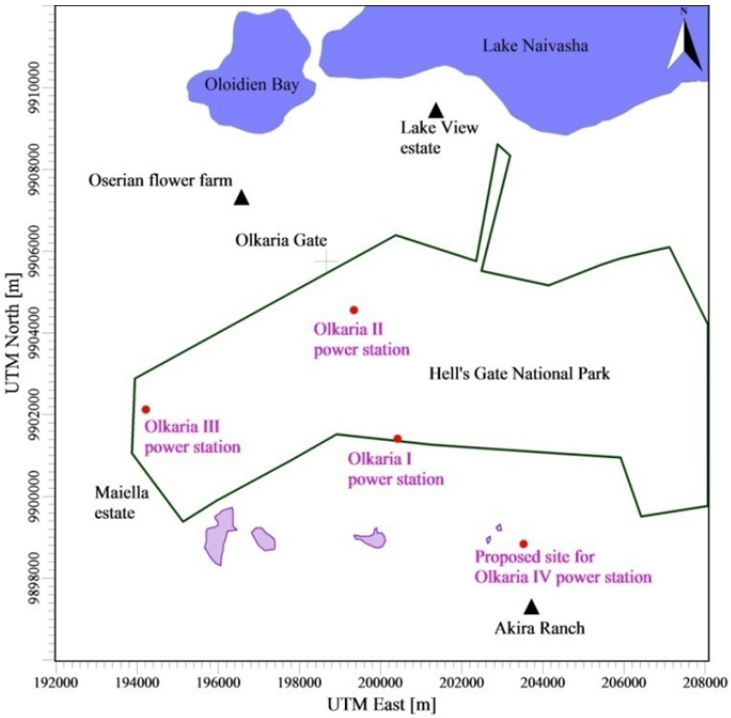

FIGURE 3: Olkaria power stations and the neighbouring communities (For co-ordinates of emission sources, see Table 3)

It is important to determine whether noise and H_2S emissions pose any significant impact for humans, flora or fauna. Air dispersion models have been used routinely in environmental impact assessments, ecological risk analysis and emergency planning. The models are also useful in properly designing and configuring sources of pollution to minimise ambient impacts (ADEQ, 2004) and effectively predict the impacts of hydrogen sulphide on both the workers inside the plants and the nearby population (Ermak et al., 1980; Gallegos-Ortega et al., 2000). Air dispersion modelling is used by many regulatory agencies as a means of assessing the impact of a facility on the air quality of the surrounding area, and to determine the compliance status. Such models are a reliable basis for developing and making decisions about environmental management and sustainability and to provide information on real-time emission abatement strategies.

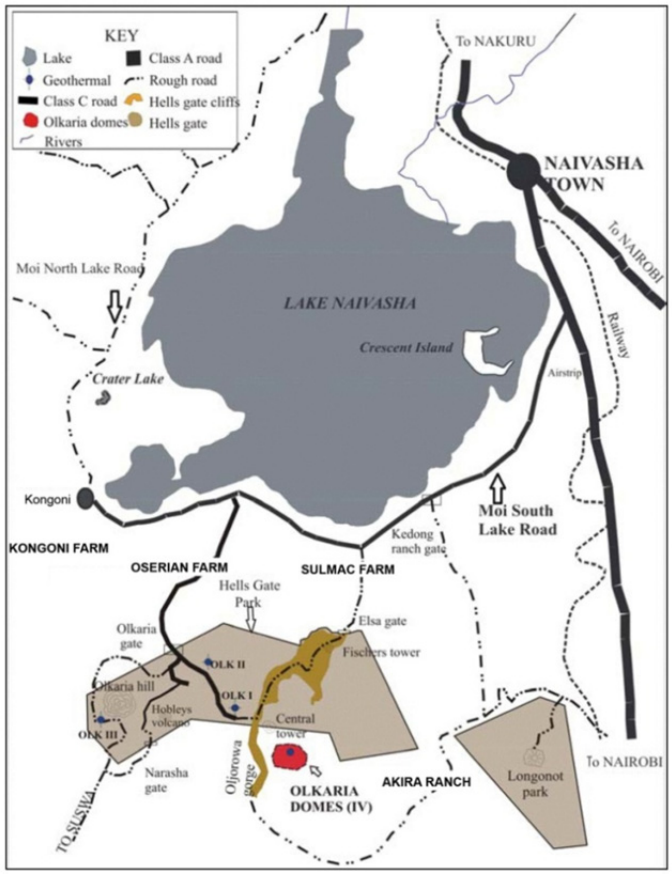

FIGURE 4: Olkaria and its vicinity (Were, 2007)

4. STUDY AREA

4.1 Location and geological setting of Olkaria

This study focuses on the Olkaria geothermal area in Kenya located on the floor of the rift valley, about 120 km northwest of Nairobi. Of particular interest is the existing Olkaria I and Olkaria II power stations and the proposed Olkaria IV power station. Figure 4 shows the location of Olkaria and the surrounding region, while Figure 5 shows the volcano-tectonic map of Olkaria.

Geothermal resources at Olkaria are associated with the Olkaria rhyolitic volcanic complex, which consists of a series of lava flows and domes, the youngest of which has been dated at about 250±100 years ago (Simiyu, 2008). Clarke et al. (1990) described the geology of Olkaria as being characterised by numerous eruptive volcanic centres of Quaternary age. The geothermal field is located within a remnant of a caldera complex intersected by N-S rifting faults. These faults are conduits for numerous eruptions that have formed pumice and ryholite domes within the Olkaria volcanic complex. The area has a thick cover of pyroclastic ash that is thought to have erupted from volcanic centres outside Olkaria, namely Suswa and Longonot. The Olkaria volcanic complex is considered to be bounded by arcuate faults forming a ring or a caldera structure. Within this structure, a magmatic heat source might be represented by intrusions at depth. Faults and fractures are prominent in the area with general N-S and E-W trends, but there are also some inferred faults striking NW-SE. Other structures in the Olkaria area include the Ol'Njorowa gorge that trends NW-SE and may represent a fault, the Ololbutot fault that trends N-S, the ENE-WSW trending Olkaria fault, the WNW-ESE trending gorge farm fault, and Olkaria fractures.

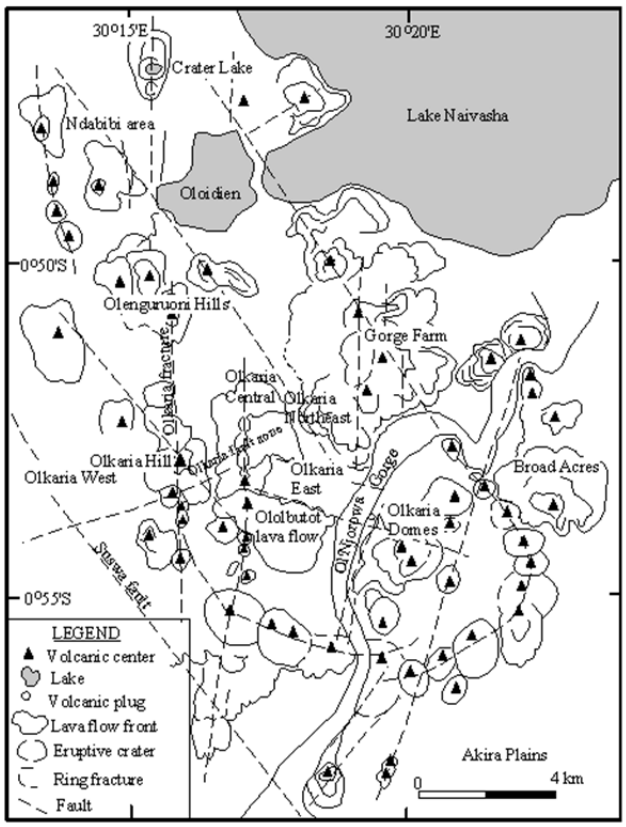

FIGURE 5: Volcano-tectonic map of Olkaria field (modified from Clarke et al., 1990)

4.2 Noise and H_2S monitoring

Near ground noise levels and H_2S concentrations are monitored in and around Olkaria I and II power stations using manually operated samplers. There are about 18 sites in total for monitoring H_2S at Olkaria I and II power stations and its neighbourhood. The sites at Olkaria I include the MV-rig workshop, power station, Olkaria I administration offices, seal pit 1, seal pit 2, well OW-10, well OW-22, scientific laboratories and a general store. At Olkaria II, identified sites include a compressor room, hot well pit unit 1, hot well pit unit 2, cooling towers, power house, Olkaria II administration offices and Kenya Wildlife Service (KWS) Olkaria gate. Monitoring is also carried out in residential areas such as Lake View and Lake Side housing estates. Figure 6 shows the monitoring sites for noise levels and H_2S concentrations.

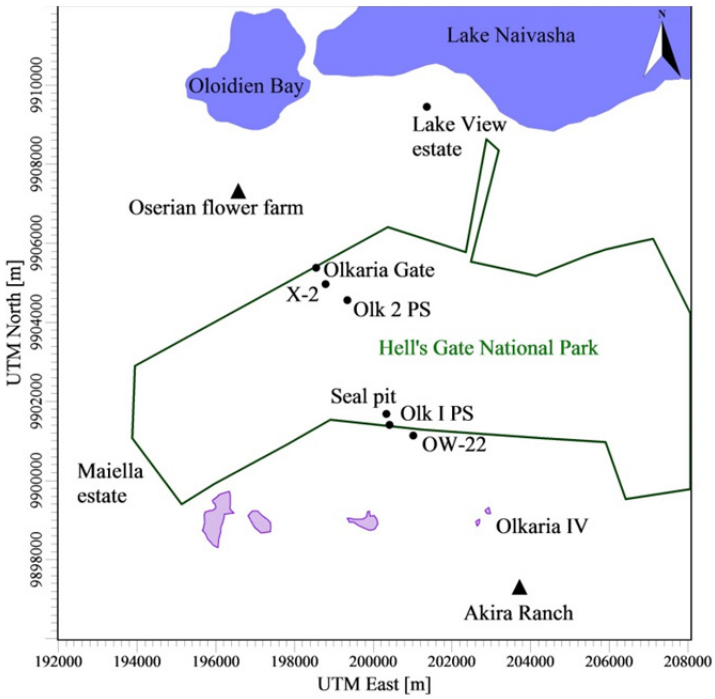

FIGURE 6: Location of noise and H_2S monitoring sites

The main sources of noise include the power house (the building that houses electricity generators and turbines), steam separators and the cooling towers, whereas the main sources of hydrogen sulphide are the cooling towers and the power house. Although there might be other sources of noise and H_2S such as from drilling operations and well testing, these are only temporary and typically last for days. Thus, the main emphasis is on the assessment of noise from the permanent operations of the power stations while H_2S sources are the cooling towers or the gas ejectors. At Olkaria I the gas ejector and the plant are essentially co-located, whereas at Olkaria II, gas ejection occurs in the cooling towers so that the actual H_2S sources in the aggregation are different for the two power stations; however, this does not change the way the H_2S modelling is undertaken.

5. METHODOLOGY

5.1 Theoretical approach to air dispersion

Air pollutant plume dispersion equations have been undertaken by numerous researchers. By performing a mass balance on a small control volume, a simplified diffusion equation, which describes a continuous cloud of material dispersing in a turbulent flow, can be written as (Macdonald, 2003):

$$\frac{\partial C}{\partial t} + U\frac{\partial C}{\partial x} = \frac{\partial}{\partial y}\left(K_y \frac{\partial C}{\partial y}\right) + \frac{\partial}{\partial z}\left(K_z \frac{\partial C}{\partial z}\right) + S \quad (1)$$

where x = Along-wind coordinate measured in wind direction from the source;
y = Cross-wind coordinate direction;
z = Vertical coordinate measured from the ground;
$C(x,y,z)$ = Mean concentration of diffusing substance at a point (x,y,z) (kg/m^3);
K_y, K_z = Diffusivities in the direction of the y- and z- axes (m^2/s);
U = Mean wind velocity along the x-axis (m/s); and
S = Source/sink term (kg/m^{3}s).

A term by term interpretation of Equation 1 is:

$\frac{dC}{dt} + U\frac{dC}{dx}$ Time rate of change and advection of the cloud by the mean wind;

$\frac{d}{dy}\left(K_y \frac{dC}{dy}\right), etc$ Turbulent diffusion of material relative to the centre of the pollutant cloud; and

S Source term which represents the net production of pollutants.

In deriving Equation 1, it is assumed that the pollutant concentrations do not affect the flow field (passive dispersion), molecular diffusion and longitudinal (along-wind) diffusion are negligible, flow is incompressible, wind velocities and concentrations can be decomposed into a mean and fluctuating component with the average value of the fluctuating (stochastic) component equal to zero, turbulent fluxes are linearly related to the gradients of the mean concentrations and the mean lateral (V) and vertical (W) wind velocities are zero.

An analytical solution to Equation 1 gives the Gaussian plume model. For a continuous point-source released at the origin in a uniform (homogenous) turbulent flow, the solution to Equation 1, as given by Macdonald (2003), is:

$$C(x,y,z) = \frac{Q}{4\pi x\sqrt{K_y K_z}} exp\left(\frac{-y^2}{4K_y(x/U)}\right) exp\left(\frac{-z^2}{4K_z(x/U)}\right) \quad (2)$$

where Q is the source pollutant emission rate.

The turbulent diffusivities K_y and K_z are unknown in most flows; in the atmospheric boundary layer, K_z is not constant, but increases with height above the ground. In addition, K_y and K_z increase with distance from the source, because the diffusion is affected by different scales of turbulence in the atmosphere as the plume grows. If we define the lateral dispersion coefficient function, σ_y, and the vertical diffusion coefficient function, σ_z , as follows (Seinfeld and Pandis, 2006):

$$\sigma_y = \sqrt{2K_y \frac{x}{U}} \; and \; \sigma_z = \sqrt{2K_z \frac{x}{U}} \tag{3}$$

then the final form of the Gaussian plume equation, for an elevated plume released at $z = H_p$ is (Seinfeld and Pandis, 2006):

$$C(x,y,z) = \frac{Q}{2\pi U_p \sigma_y \sigma_z} exp\left(-\frac{y^2}{2\sigma_y^2}\right)\left[exp\left\{-\frac{(z-H_p)^2}{2\sigma_z^2}\right\} + exp\left\{-\frac{(z+H_p)^2}{2\sigma_z^2}\right\}\right] \tag{4}$$

In this expression, a second z-exponential term has been added to account for the fact that a pollutant cannot diffuse downward through the ground at $z = 0$, but is assumed to be reflected. This "image" term can be visualised as an equivalent source located at $z = -H_p$ below the ground.

Equation 4 is the Gaussian plume formula for a continuous point source. The plume height H_p is the sum of the actual stack height H_s plus any plume rise ΔH_s due to initial buoyancy and momentum of the release. The wind speed U_p is taken to be the mean wind speed at the height of the stack. Considering concentrations at ground level (where receptors are) and assuming $= 0$, we obtain (Macdonald, 2003):

$$C(x,y,z=0) = \frac{Q}{\pi U_p \sigma_y \sigma_z} exp\left(-\frac{y^2}{2\sigma_y^2}\right) exp\left(-\frac{H_p^2}{2\sigma_z^2}\right) \tag{5}$$

A general non-Gaussian model, which allows for vertical variation, is expressed as:

$$C(x,y,z) = \frac{Q}{\sqrt{2\pi} U_p \sigma_y} exp\left(-\frac{y^2}{2\sigma_y^2}\right) f(z) \tag{6}$$

Here $f(z)$ is a normalized function that describes the vertical distribution of material in the plume.

The rate of transfer of a pollutant through any vertical plane downwind from the source is a constant steady state, and this constant should equal the emission rate of the source, Q. Thus:

$$\iint_{y,z} CU \, dydz = Q \tag{7}$$

where the integration is performed over the y-z plane, perpendicular to the plume axis.

5.2 Available data and sources

The AERMOD dispersion model (Cimorelli et al., 2004) was used to simulate H_2S dispersion and concentrations due to emissions from the existing Olkaria I and Olkaria II power plants and the

proposed Olkaria IV power plant. The AERMOD dispersion model requires surface data on meteorology (wind speed (m/s), wind direction (degrees), dry bulb temperature (°C), relative humidity (%), station pressure (mbar), opaque cloud cover (tenth), cloud ceiling height (m), and global horizontal radiation (W/m^2)), atmospheric stability obtained from upper air soundings, surface characteristics (surface roughness, Bowen ratio and albedo) and information about the source being modelled, including pollutant emission rate, location and exit velocity. Surface meteorological data was obtained from the Environment unit of KenGen, Olkaria. The data was produced by an automatic weather station located at X-2, about 500 m northwest of the Olkaria II power plant, for the period November 2003 to September 2006. For modelling purposes, surface meteorology data for the period 1st to 30th November 2003 was used since it was complete. Upper air data was available from Dagoretti meteorological weather station, located at latitude 1.30°S and 36.75°E, which is more than 120 km from the area of interest. Since the upper air sounding station was located far from the area of interest, upper air data was estimated by the model using the available surface meteorological data. A Bowen ratio of 4, albedo of 0.28 and surface roughness of 0.3 were used in the modelling. Table 3 gives a description of the emission parameters that were used to model dispersion.

In Olkaria, the non-condensable gases such as H_2S, CO_2, CH_4 and N_2 present in geothermal fluid (Sinclair Knight and Partners, 1994) are disposed of by discharging them into cooling tower fans for dispersal into the atmosphere. There is a difference between Olkaria I and Olkaria II power stations due to the ways in which they dispose of waste hydrogen sulphide. Olkaria II power station discharges the non-condensable H_2S with evaporative emissions in the cooling tower plume, whereas Olkaria I power station discharges the H_2S through gas ejectors located in the main power station building. The cooling tower plumes have a substantial plume-rise compared with the plume-rise from the gas ejectors (Sinclair Knight and Partners, 1994). However, for modelling purposes, the two power plants have been treated in the same way.

5.3 Model descriptions

The selection of an air dispersion model depends on many factors such as the nature of the pollutant, characteristics of emission sources and the relationship between the emission source and the receptor. Other factors influencing model selection include meteorological and topographic complexities of the area, complexity of the source distribution, spatial scale and resolution required for the analysis, level of detail and accuracy required for the analysis, and averaging times to be modelled. Some of the well known models include ISCST3, AERMOD, ASPEN, CALPUFF, UTM-TOX, and CAMx. In this study, AERMOD was applied to model H_2S dispersion.

AERMOD stands for AERMIC Model, where AERMIC is the **A**merican Meteorological Society/**E**PA **R**egulatory **M**odel **I**mprovement **C**ommittee. AERMOD was developed in 1995, reviewed in 1998 and formally proposed by the United States Environmental Protection Agency (US EPA) as a replacement for the Industrial Source Complex Short Term model (ISC-ST3) in 2000 (Bluett et al., 2004).

A detailed description of AERMOD was given by Cimorelli et al. (2004). AERMOD is a steady-state plume model. In the stable boundary layer (SBL), it assumes the concentration distribution to be Gaussian both vertically and horizontally. In the convective boundary layer (CBL), the horizontal distribution is also assumed to be Gaussian, but the vertical distribution is described with a bi-Gaussian probability density function (pdf). Additionally, in the CBL, AERMOD monitors "plume lofting", whereby a portion of plume mass, released from a buoyant source, rises to and remains near the top of the boundary layer before becoming mixed into the CBL. AERMOD also tracks any plume mass that penetrates into the elevated stable layer, and then allows it to re-enter the boundary layer when and if appropriate. For sources in both the CBL and the SBL, AERMOD treats the enhancement

TABLE 3: Emission parameters used to model dispersion from existing Olkaria I and Olkaria II power stations and the proposed Olkaria IV power station (Holmes Air Sciences, 2009)

Parameter	**Olkaria I**		**Olkaria II (Units 1 and 2)**		**Olkaria II (Unit 3)**		**Proposed Olkaria IV (Units 1 and 2)**	
Height of emission point above grade (m)	19		16		19		19	
Height of grade above sea level (m)	1932		2005		2005		2035	
Exit velocity (m/s)	20		9.2		8.6		8.6	
Exit temperature (K)	375		304		303		303	
Diameter of discharge point at tip (m)	0.2		9.14		9.64		9.64	
Mass emission rate of H_2S for each of the 3 emission points for Olkaria I, 12 emission points for Olkaria II, and 8 emission points for Olkaria IV, respectively (g/s)	4.46		3.55		3.55		7.1	
Coordinates of discharge points (in UTM, zone 37 south of the equator)	Easting 200420 200412 200404	Northing 9901480 9901500 9901525	Easting 199365 199370 199376 199382 199387 199393 199399 199404	Northing 9904727 9904717 9904708 9904699 9904689 9904680 9904670 9904661	Easting 199356 199349 199342 199336	Northing 9904744 9904755 9904766 9904777	Easting 203538 203533 203527 203521 203516 203510 203504 203499	Northing 9898811 9898820 9898830 9898839 9898849 9898858 9898867 9898877

of lateral dispersion resulting from plume meander. AERMOD handles the computation of pollutant impacts in both flat and complex terrain within the same modelling framework. Using a relatively simple approach, AERMOD incorporates current concepts about flow and dispersion in complex terrains. Where appropriate, the plume is modelled as either impacting and/or following the terrain. The model also has the ability to characterise the Planetary Boundary Layer (PBL) through both surface and mixed layer scaling (Cimorelli et al., 2004).

5.3.1 AERMET

AERMET is the meteorological pre-processor of AERMOD. The input data to AERMET, as described by Cimorelli et al. (2004), consists of surface roughness, albedo and Bowen ratio, plus standard meteorological observations including wind speed, wind direction, temperature and cloud cover. AERMET then calculates the PBL parameters which include friction velocity (u_*), Monin-Obukhov length (L), convective velocity scale (w_*), temperature scale (θ_*), mixing height (z_i), and surface heat flux (H). These scaling parameters are used to construct vertical profiles of wind speed (u), lateral and vertical turbulent fluctuations (σ_x, σ_y), potential temperature gradient $(d\theta/dz)$, and potential temperature (θ). Detailed mathematical expressions of these PBL parameters are described by Cimorelli et al. (2004).

5.3.2 AERMAP

AERMAP is the terrain pre-processor of AERMOD and uses gridded terrain data to calculate a representative terrain-influence height *(hc*) for each receptor with which AERMOD computes receptor specific *Hc* values. AERMOD handles the computation of pollutant impacts in both flat and complex terrain within the same modelling framework (Cimorelli et al. (2004)) as illustrated in Figure 7. In complex terrain, AERMOD incorporates the concept of the dividing streamline for stability-stratified conditions. Where appropriate, the plume is modelled as a combination of two limiting cases: a horizontal plume (terrain impacting) and a terrain-following (terrain responding) plume. In stable flow, a two-layer structure develops in which the lower layer remains horizontal while the upper layer tends to rise over the terrain. In neutral and unstable conditions *Hc* = 0. AERMOD captures the effect of flow above and below the dividing streamline by weighting the plume concentration associated with two possible extreme states of the boundary layer: horizontal plume and terrain-following. The relative weighting of a horizontal plume and terrain-following depends on the degree of atmospheric stability, the wind speed and the plume height relative to the terrain. The weighting of the two plume states depends on the amount of mass residing in each state. This mass partitioning is based on the relationship between the critical dividing streamline height (*Hc*) and the vertical concentration distribution at a receptor.

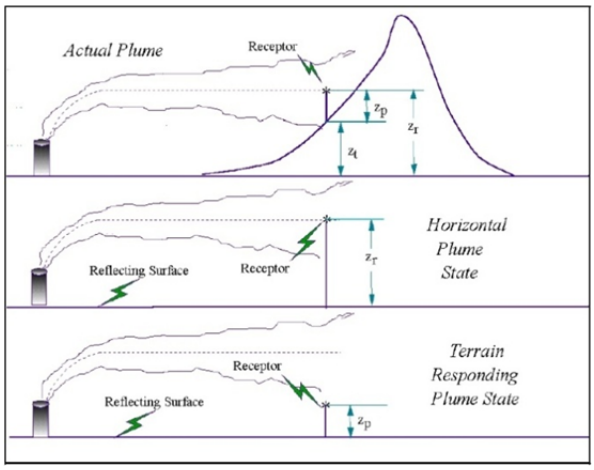

FIGURE 7: AERMOD horizontal plume state and terrain-following state approaches (Cimorelli et al., 2004)

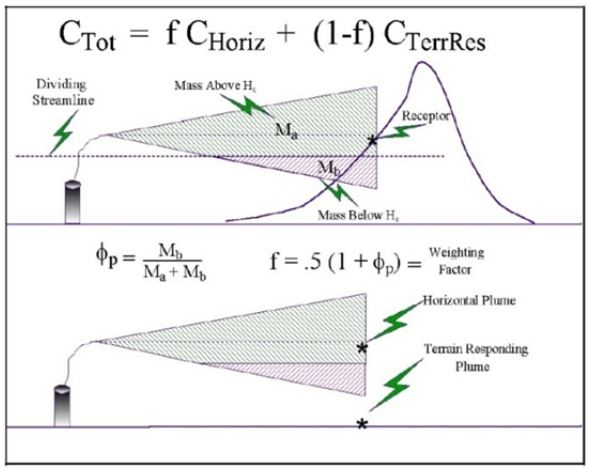

FIGURE 8: Treatment of terrain in AERMOD; construction of the weighting factor used in calculating total concentration (Cimorelli et al., 2004)

During convective conditions the concentration at an elevated receptor is the average of the contributions from the two states. As plumes above *Hc* encounter terrain and are deflected vertically, there is also a tendency for plume material to approach the terrain surface and to spread out around the sides of the terrain. To simulate this, concentration estimates always contain a component from the horizontal state and, hence, under no condition is the plume allowed to completely approach the terrain-following state. For flat terrain, the contributions from the two states are equal in value and are equally weighted. Figure 8 illustrates how the weighting factor is constructed and its relationship to the estimate of concentrations as a weighted sum of two limiting plume states.

The modelling used the default regulatory dispersion option for H_2S concentration output and assumed a flat terrain height. The Universal Transverse Mercator (UTM) projection for zone 37 south of the equator was employed using the world geodetic system of 1984 (WGS-84). The prediction of H_2S concentrations was simulated using 1-hour average, 8-hour average and 24-hour average time periods. A uniform Cartesian grid spacing of 200 m by 200 m was considered over a length of 16 km by 16 km extending from E192000 m to E208000 m and N9896000 m to N9912000 m.

6. RESULTS

6.1 Temporal variation of meteorology, noise and hydrogen sulphide concentrations at Olkaria

Figure 9 shows the monthly mean air temperature and relative humidity from meteorological station X-2, Olkaria. Measurements were made at twice-daily intervals: 09:00 and 15:00 local standard time. The maximum temperature recorded in the area ranged between 21.6 and 28.5°C, with a mean value of 24.8°C. Minimum temperature in the area ranged between 8.3 and 14.1°C, with a mean value of 11.1°C. Relative humidity at the station ranged between 55.2 and 86.0%, with a mean value of 73%. Thus, the temperatures and relative humidity showed relatively modest seasonal variations.

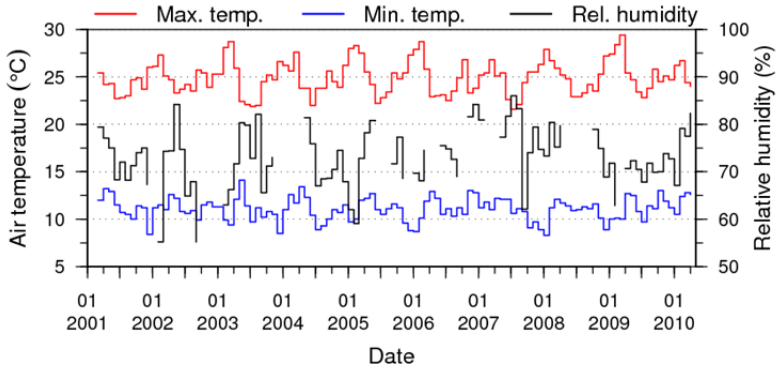

FIGURE 9: Monthly mean air temperature and relative humidity from meteorological station X-2, Olkaria

Figure 10 shows the mean monthly variation of noise at Olkaria I power station and its vicinity. Noise level data was collected from March 1995 to April 2010. The main source of noise at Olkaria I is the power station building which houses the turbines and generators and, as indicated in Figure 10, noise levels at the monitoring site near the power station occasionally exceeded the recommended WHO limit of 85 dB(A). However, moving farther away from the source, noise levels decayed as illustrated by measurements mostly below 75 dB(A) recorded at the administration block and at the KWS gate monitoring sites. Noise levels in the Lake View residential area were below 50 dB(A), the limit set by the Kenyan National Environment Agency.

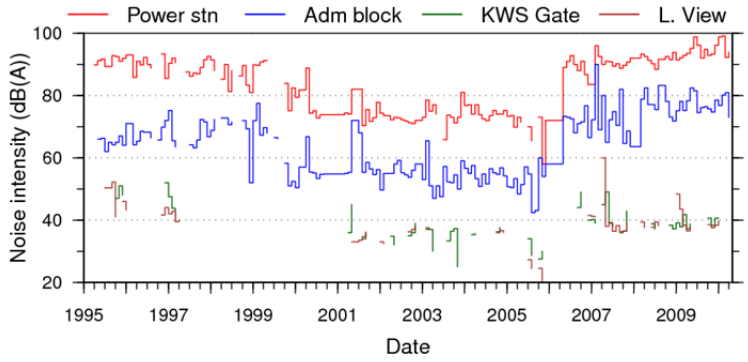

FIGURE 10: Mean monthly variation of noise at Olkaria I and its vicinity

Figure 11 shows the mean monthly variation of noise at Olkaria II power station. Noise data at Olkaria II power station were collected from September 2003 to April 2010. The noise levels at Olkaria II power station were within the WHO limit of 85 dB(A), as illustrated by measurements taken at the monitoring sites at the power station, the cooling tower and the Olkaria II administration block. Although the overall noise level at Olkaria II was within permitted limits, Figure 11 shows a pronounced increase in intensity from mid 2006 onwards. A comparison of

FIGURE 11: Mean monthly variation of noise at Olkaria II

Figures 10 and 11 indicates that noise intensity was relatively higher at Olkaria I than at Olkaria II. This might be attributed to the newer technology in use at Olkaria II.

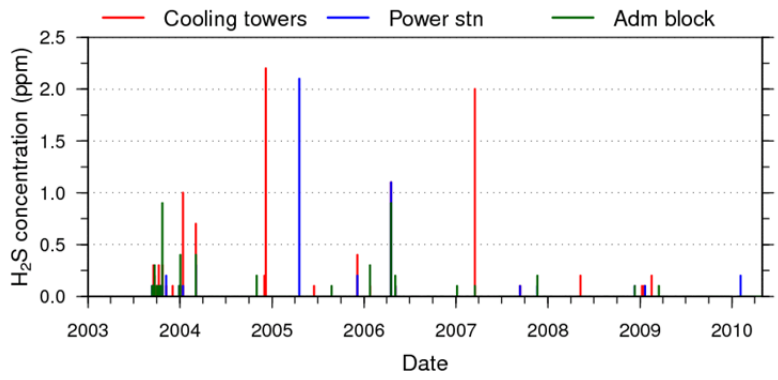

FIGURE 12: Daily variation of H_2S at Olkaria II

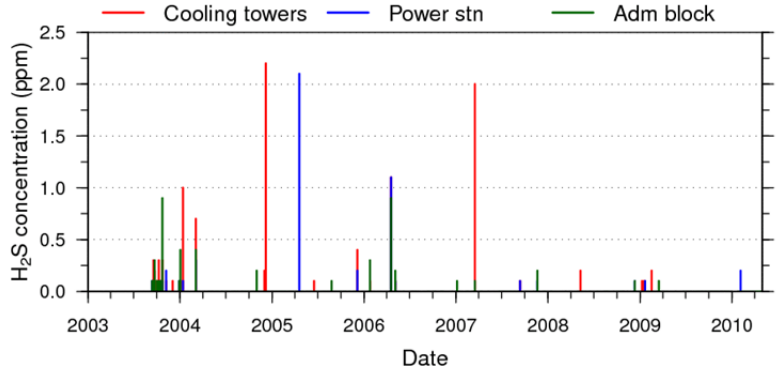

FIGURE 13: Daily variation of H_2S at Olkaria I

H_2S emissions from Olkaria I and Olkaria II power stations were monitored from April 1997 and September 2003 to April 2010, respectively. Figures 12 and 13 show the daily variations of H_2S concentrations at Olkaria II and Olkaria I power stations. The highest recorded value of H_2S at Olkaria II was 2.2 ppm while at Olkaria I, the highest recorded value was 4.4 ppm. Thus, H_2S concentrations at Olkaria I and Olkaria II power stations were below the National Institute of Occupational Safety and Health (NIOSH) standards of 10 ppm averaged over a 24-hour period for employees working eight hours per day for five days in a week. Similarly, H_2S concentrations outside the plant boundaries were far below the WHO (2000) limit of 0.1 ppm. H_2S concentrations at Olkaria II were relatively low, occasionally below the detection threshold. However, this was not the case with Olkaria I power station where H_2S emission was evident (Figure 13) and the detection threshold of 0.0047 ppm (Chambers and Johnson, 2009) was frequently exceeded.

6.2 Spatial variation of noise and hydrogen sulphide at Olkaria

The spatial variations of the noise levels and H_2S concentrations emanating from Olkaria I and Olkaria II power stations are shown in Figures 14 to 17. The spatial variation of noise at Olkaria I and Olkaria II power stations indicates that noise was emitted mainly from the cooling towers and the power house, spreading to the surrounding areas in a decaying logarithmic pattern. Noise levels near Olkaria II power station were in the range of 80 dB(A), and decreased with distance so that noise levels at the

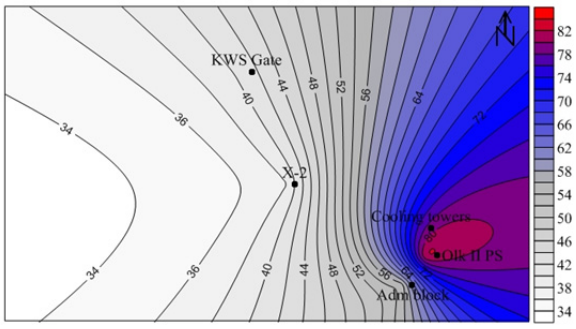

FIGURE 14: Spatial variation of noise (dB(A)) at Olkaria II

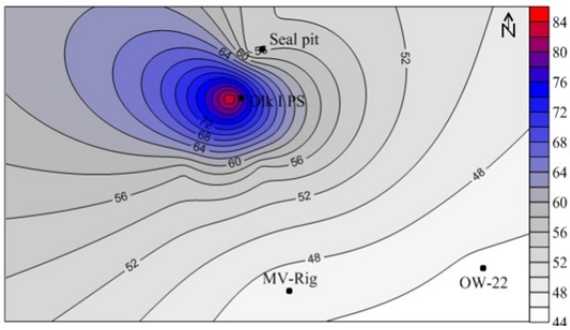

FIGURE 15: Spatial variation of noise (dB(A)) at Olkaria I

KWS gate, about 600 m away, were in the range of 42 dB(A), as indicated in Figure 14. Figure 15 shows the spatial variation of noise at Olkaria I power station and its surroundings.

The annual average concentration of hydrogen sulphide near Olkaria II power plant was in the range of 0.03 ppm, and dispersed such that the concentration at the KWS gate, about 600 m from Olkaria II power station, was 0.002 ppm (Figure 16). Relatively high concentrations of hydrogen sulphide were recorded at Olkaria I, as indicated in Figure 17, with the highest concentration of 0.36 ppm recorded at close proximity to the power station.

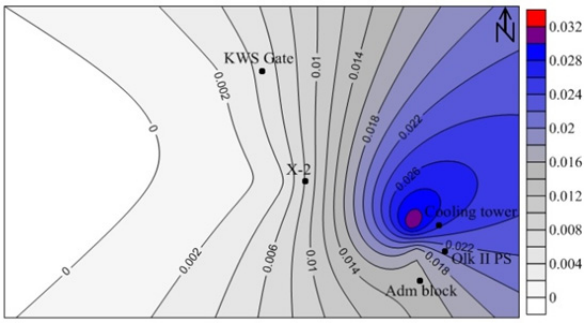

FIGURE 16: Spatial variation of H_2S (ppm) at Olkaria II

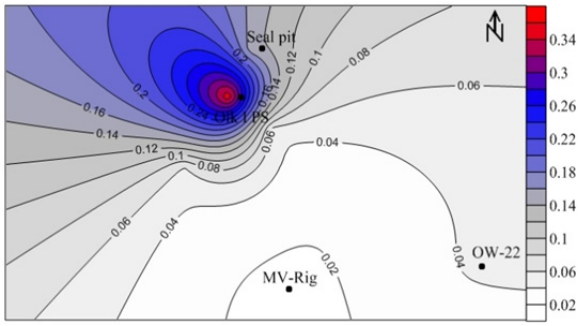

FIGURE 17: Spatial variation of H_2S (ppm) at Olkaria I

6.3 Wind distribution at Olkaria

Figure 18 shows the seasonal windroses for the Olkaria area for the periods (a) December to February (b) March to May (c) June to July and (d) September to November. These periods represent the four main seasons in Kenya. Automatic wind speed and wind direction data collected from November 2003 to September 2005 were used to plot the windroses. Figure 18 indicates that the general wind pattern at Olkaria is southeast in all seasons except summer (December-January - February) when the wind pattern randomised, characterised by southeasterly and northwesterly directions.

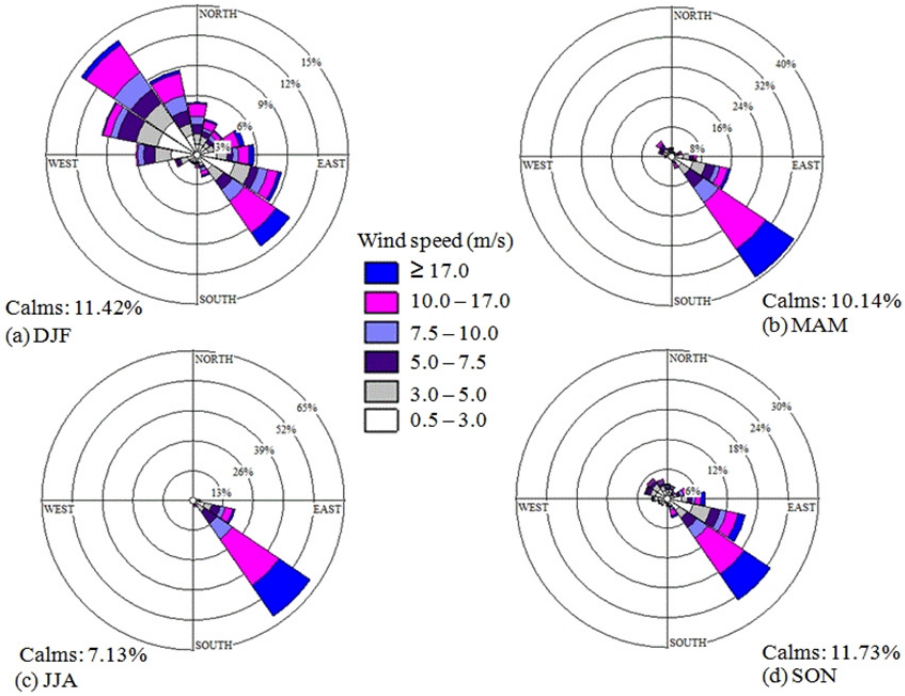

FIGURE 18: Seasonal windroses for X-2 weather station, Olkaria; (a) December to February (b) March to May (c) June to July (d) September to November

6.4 Modelling results from AERMOD

6.4.1 Air dispersion results from the existing Olkaria I (Units 1, 2, 3) and Olkaria II (Units 1, 2, 3) power stations

Air dispersion results for Olkaria I (Units 1, 2 and 3) and Olkaria II (Units 1, 2 and 3) generally predicted that high concentrations of H_2S would occur near the power plants; the concentration values for Olkaria I measured higher than those for Olkaria II.

Figure 19 shows that the highest predicted H_2S concentrations, averaged over a one-hour period, equalled 1356 µg/m^3 (0.963 ppm), due to emissions from the three units of Olkaria I and the three units of Olkaria II. This highest concentration occurred at E199400 m and N99046000 m, which is close to the Olkaria I power station. The plume concentrated about 500 m from the power plant and spread mainly eastwards as it decayed so that at a distance of 500 m, the concentration was 242 µg/m^3 (0.172 ppm).

H_2S concentrations averaged over 8-hour periods indicated that the highest concentration equalled 297 µg/m^3 (0.211 ppm), sourced at E199400 m and N9904800 m, which is near Olkaria I power station (Figure 20). The plume emitted from Olkaria I power station dispersed to the northeast; the values were relatively small so that at a distance of about 600 m from the station, the concentrations were 60 µg/m^3 (0.043 ppm). At Olkaria II power station, H_2S concentrations were lower than at Olkaria I, and concentrated near the station. The highest 8-hour average concentration

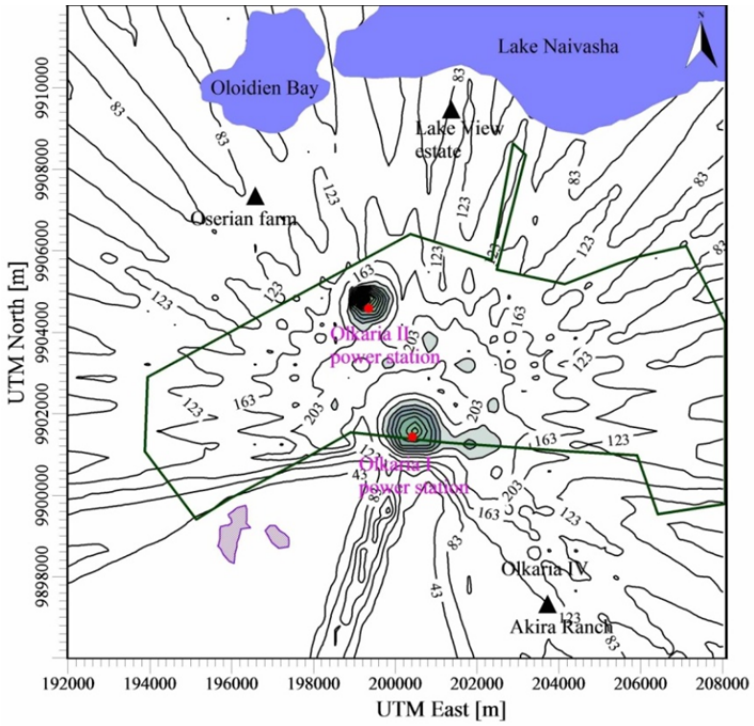

FIGURE 19: Predicted 1-hour averaged H_2S concentrations (µg/m^3) due to emissions from the existing Olkaria I (Units 1, 2, 3) and Olkaria II (Units 1, 2, 3) power stations

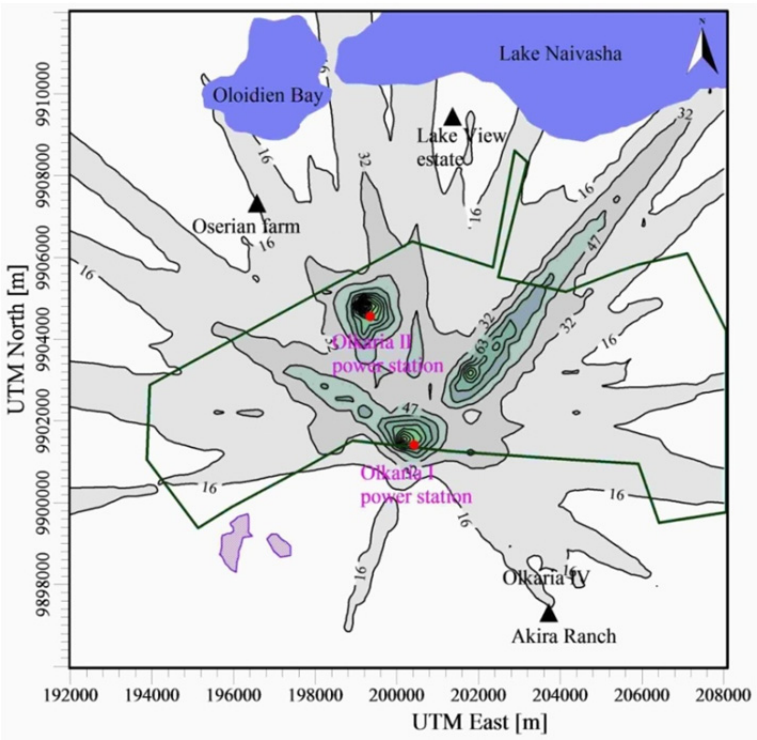

FIGURE 20: Predicted 8-hour averaged H_2S concentrations (µg/m^3) due to emissions from the existing Olkaria I (Units 1, 2, 3) and Olkaria II (Units 1, 2, 3) power stations

value at Olkaria II equalled 219 µg/m^3 (0.155 ppm) and dispersed uniformly so that at a distance of about 500 m, the concentration was 47 µg/m^3 (0.033 ppm).

For the case of 24-hour averaged concentrations, the highest predicted H_2S concentration equalled 118 µg/m^3 (0.0838 ppm), located at E200200 m and N9901600 m which is close to Olkaria I power station (Figure 21). The plume from Olkaria I power station spread northeast; at a distance of 400 m northeast of the station, the concentration was in the range of 50 µg/m^3 (0.035 ppm). At Olkaria II power station, the highest H_2S concentration was 99 µg/m^3, decaying to a concentration of 50 µg/m^3 at 300 m from the station. The dispersion model indicated that 24-hour average H_2S concentrations due to emissions from Olkaria I and Olkaria II power stations were far below the WHO threshold limit value of 150 µg/m^3 (0.1 ppm) beyond the power station boundary (WHO, 2000).

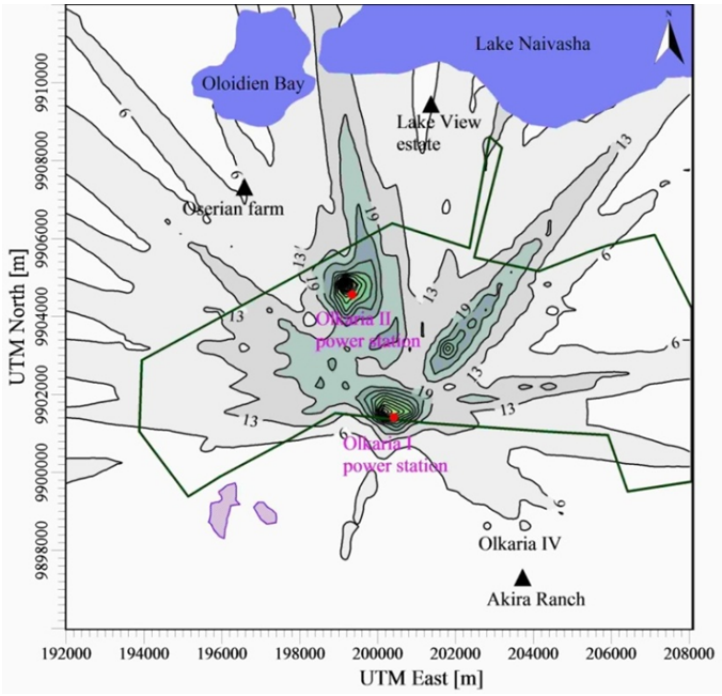

FIGURE 21: Predicted 24-hour averaged H_2S concentrations (µg/m^3) due to emissions from the existing Olkaria I (Units 1, 2, 3) and Olkaria II (Units 1, 2, 3) power stations

6.4.2 Air dispersion results from the existing Olkaria I (Units 1, 2, 3), Olkaria II (Units 1, 2, 3) and the proposed Olkaria IV (Units 1, 2) power stations

H_2S dispersion results for the two existing power plants, Olkaria I (units 1, 2, 3) and Olkaria II (units 1, 2, 3), and for the proposed 2 units of Olkaria IV indicated 1-hour averaged concentrations of 1948 µg/m^3 (1.383 ppm) at E203400 m and N9898800 m; this was in close proximity to the proposed Olkaria IV power station (Figure 22). At a distance of 500 m from the Olkaria IV power plant, the 1-hour average predicted a concentration of 340 µg/m^3 (0.241 ppm). The dispersion model indicated that the residential area about 4 km southwest of Olkaria I had minimal or no health impacts due to emissions from the three power plants.

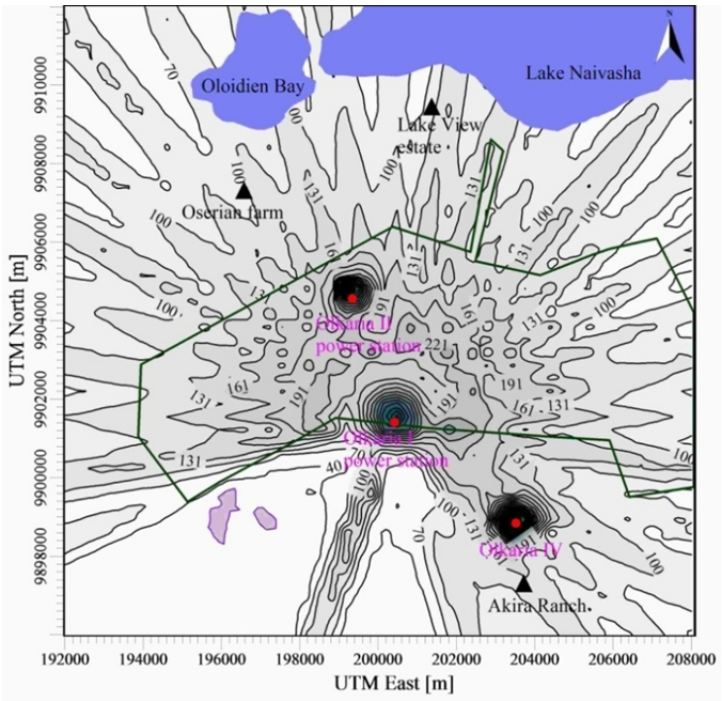

FIGURE 22: Predicted 1-hour averaged H_2S concentrations (µg/m^3) due to emissions from the existing Olkaria I (Units 1, 2, 3), Olkaria II (Units 1, 2, 3) and the proposed Olkaria IV (Units 1 and 2) power stations

Figure 23 shows 8-hour averaged H_2S concentration levels due to emissions from the existing two power plants (Olkaria I and Olkaria II) and the proposed power plant (Olkaria IV). The plume dispersion model indicated that the highest 8–hour averaged hydrogen sulphide concentration of 644 µg/m^3 (0.457 ppm) would be in close proximity to Olkaria IV (E203400 m, N9898800 m). A zone of H_2S was also noted northeast of Olkaria I power station, attaining a maximum ground level concentration of 130 µg/m^3 (0.092 ppm) at about 2 km from the station.

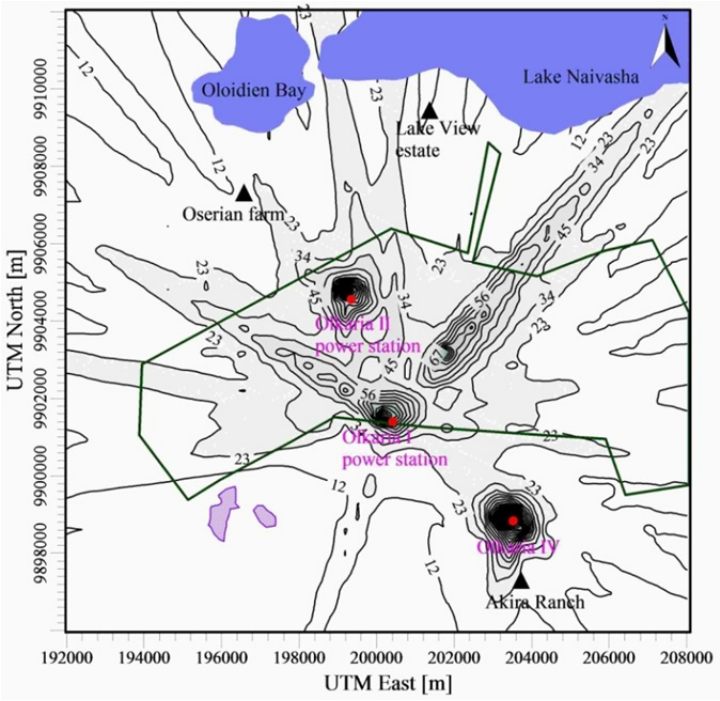

FIGURE 23: Predicted 8-hour averaged H_2S concentrations (µg/m^3) due to emissions from the existing Olkaria I (Units 1, 2, 3), Olkaria II (Units 1, 2, 3) and the proposed Olkaria IV (Units 1 and 2) power stations

Figure 24 shows the predicted 24-hour averaged concentration of H_2S due to emissions from Olkaria I (units 1, 2, 3), Olkaria II (units 1, 2, 3) and Olkaria IV (units 1, 2) power plants. The dispersion model estimated the highest concentration as 410 µg/m^3 (0.291 ppm). A plume of H_2S spread northeast of Olkaria I and north of Olkaria II. The model predicted that the residential area extending from 500 m south and southwest of Olkaria I would be free of atmospheric pollution from the three power plants, while settlements inside the power plant boundary of the proposed Olkaria IV were within the boundary for 150 µg/m^3 H_2S concentration.

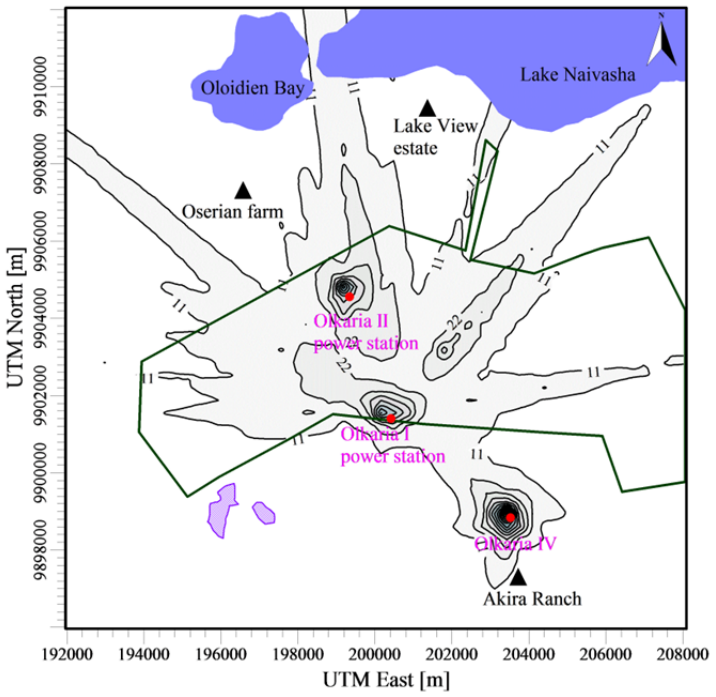

FIGURE 24: Predicted 24-hour averaged H_2S concentrations (µg/m^3) due to emissions from the existing Olkaria I (Units 1, 2, 3), Olkaria II (Units 1, 2, 3) and the proposed Olkaria IV (Units 1 and 2) power stations

The addition of Olkaria IV power plant to the existing Olkaria I and Olkaria II power plants will neither impact Akira ranch nor the Oserian farm or Lake View estate. As shown in Figure 24, the proposed site for Olkaria IV power station is located on private land, outside the Kenya Wildlife Service (KWS) boundary. According to WHO guidelines (WHO, 2000), 24-hour averaged H_2S concentrations should not exceed 150 µg/m^3 (0.1 ppm) beyond the immediate power station boundary. If the WHO assessment criterion is to be met, then it implies a relocation plan should exist for some human settlements residing within the power plant boundaries of the proposed Olkaria IV power station.

7. IMPLICATIONS

The highest predicted H_2S concentration for 1-hour averaged values from the existing Olkaria I and II power plants was 1356 μg/m^3 (0.963 ppm). According to the dispersion simulation, the addition of Olkaria IV power station to the existing power stations would increase the highest 1-hour concentration to 1948 μg/m^3 (1.383 ppm). It was predicted that this worst condition would be concentrated within the plant boundary and would decrease rapidly with distance from the power plant. Thus, H_2S concentrations due to exploitation of Olkaria IV power station would have negligible impacts on the surrounding communities located outside the plant boundary. Predicted H_2S concentrations, using 8-hour and 24-hour averages due to exploitation of Olkaria I, Olkaria II and Olkaria IV power stations, did not exceed 150 μg/m^3 (0.1 ppm) beyond the plant boundaries. Hence, the more stringent WHO (2000) threshold limit of 0.1 ppm for a 24-hour period would not be exceeded outside the plant boundary. The predicted concentrations due to exploitation of the three power plants were also far below the less stringent standards set by the National Institute for Occupational Safety and Health (NIOSH); by their criterion, air quality standards should not exceed 10 ppm (14,000 μg/m^3) over an eight hour period for employees working 40 hours per week (Webster, 1995).

Generally, the highest predicted H_2S concentrations at Olkaria were close to the main gas emissions, and decreased rapidly with distance. A similar dispersion pattern has been reported both in Kenya (Marani et al., 2000) and in Sousaki, Greece (Alessandro et al., 2009). The concentrations were predicted to be too low to affect vegetation outside the plant boundaries; that is, concentrations outside the plant boundaries were less than 0.03 ppm (42.0 μg/m^3) averaged over a 24-hour period. This is supported by earlier studies carried out in the study area to assess health impacts to vegetation due to H_2S emissions arising from Olkaria I and Olkaria II power stations (Kubo and Kollikho, 2001). Similarly, there is no danger to human life or the environment since 0.1 ppm is not exceeded outside the plant boundary using 24-hour averaging. Although no health impacts were predicted to occur, as stated earlier, the model predicted that odour which is a nuisance would be presently detectable over a wide area (Figures 21 and 24) as indicated by predicted H_2S concentrations above the detection threshold of 0.0047 ppm (6.58 μg/m^3).

Plume spread was more distributed at Olkaria I than at Olkaria II power station and, similarly, H_2S concentrations were more pronounced at the former than at the latter. Thus, it can be concluded that disposing of H_2S emissions through cooling tower plumes, as is done at Olkaria II, is an improved discharging method, and will achieve much greater plume rise than when discharging the gas through gas ejectors as is the case at Olkaria I.

8. CONCLUSIONS AND RECOMMENDATIONS

Noise assessment and H_2S dispersion measurements were carried out in Olkaria. The spatial and temporal variation of noise indicated that the levels fell within the WHO limits near the power station boundary. In rare cases where the limit was exceeded, especially at the Olkaria I power station, the use of personal protective equipment such as ear muffs is recommended. Noise levels in residential areas did not exceed the limits set by the Kenyan National Environment Agency.

Predictions of H_2S concentrations were undertaken by considering two cases: (1) predicting concentrations due to emissions from the existing Olkaria I and Olkaria II power stations and (2) predicting concentrations due to emissions from the existing Olkaria I and Olkaria II power stations and the proposed Olkaria IV power station. These two cases were simulated for 1-hour, 8-hour and 24-hour averages. In all cases of 1-hour, 8-hour and 24-hour averaging scenarios, the predicted hydrogen sulphide concentrations were less than 10 ppm (14,000 μg/m^3), the threshold for workers according to the National Institute for Occupational Safety and Health (NIOSH). In general, the

averaged concentrations were high near the emission sources and were diluted depending on weather conditions, especially temperature, wind speed and direction. Generally, the predicted concentrations due to emissions from Olkaria I and Olkaria II power plants were below 0.1 ppm (150 $\mu g/m^3$) outside the power plant boundary. The AERMOD model captured the main features of H_2S dispersion at Olkaria, and used them to predict H_2S concentrations due to the existing Olkaria I and Olkaria II power plants and the proposed Olkaria IV power plant. The model predicted relatively high H_2S concentrations within the plant boundary, decreasing rapidly farther away from the power station such that concentrations at 500 m away would cause no significant impacts to humans, flora or fauna. Similar conclusions due to the exploitations of Olkaria I and Olkaria II power stations were reached by Marani et al. (2000) who studied H_2S concentrations around the Olkaria field and found no significant impacts to the environment.

The AERMOD dispersion model is a useful tool that may be employed in environmental and social impact assessments for new geothermal developments and for environmental audits of existing power plants, and can be used in decision-making based on sound theoretical grounds. The accuracy of the predicted modelling results is based on the quality of the input data used, especially meteorological data. Hence, well-equipped automatic weather stations and a high-quality database should be in operation for effective dispersion modelling.

ACKNOWLEDGEMENTS

I am greatly indebted to the United Nations University Geothermal Training Programme (UNU-GTP) and the Government of Iceland for awarding me the fellowship to undertake the six months specialised training in geothermal research. I wish to thank my employer, Kenya Electricity Generating Company Ltd. (KenGen) for granting me sabbatical leave to attend the training. Special thanks go to the UNU-GTP Director, Ingvar B. Fridleifsson, and the Deputy-Director, Lúdvík S. Georgsson. I cannot forget crucial contributions made by other UNU-GTP staff including Thórhildur Ísberg, Dorthe H. Holm, Markús A.G. Wilde and Ingimar G. Haraldsson. My sincere appreciation goes to my supervisor, Dr. Matthew J. Roberts, for his wise ideas, guidance and support. Earnest appreciation goes to the UNU-GTP class of 2010 for their memorable co-operation. Finally, I express my deepest gratitude to my workmates, friends, relatives and my family. To my dear wife and daughter, thanks for your encouragement, sacrifice, and unconditional love during my six months of study. Above all, I glorify the Mighty God for His love, care and mercy that has seen me to this point.

REFERENCES

ADEQ (Arizona Department of Environmental Quality), 2004: *Air dispersion modeling guidelines for Arizona air quality permits.* Air assessment section, air quality division, Arizona Department of Environmental Quality, December 2004, Arizona, 63 pp.

Alessandro, L., Brusca, L., Kyriakopoulos, K., Michas, G., and Papadakis, G., 2009: Hydrogen sulphide as natural air contaminant in volcanic/geothermal areas: the case of Sousaki, Corinthia-Greece. *Environ. Geol., 57*, 1723-1728.

Anderson, I., 1991: Blowout blights future of Hawaii's geothermal power. *New Sci., 17, 1778,* 17.

Babisch, W., 2000: Traffic noise and cardiovascular disease: Epidemiological review and synthesis. *Noise Health, 2*, 9-32.

Bluett, J., Gimson, N., Fisher, G., Heydenrycn, C., Freeman, T., and Godfrey, J., 2004: *Good practice guide for atmospheric dispersion modelling.* Ministry of Environment, Manatū Mō Te Taiao, Wellington, New Zealand, webpage: *www.mfe.govt.nz*, 152 pp.

Chambers, T., and Johnson, J.A., 2009: *Environmental mitigation monitoring: Hydrogen sulphide (H_2S) gas dispersion potentials and release scenarios of Pacific OCS region's oil & gas platforms and pipelines located in the Santa Barbara channel and Santa Maria basin, California*. MMS OCS, report 2009-021, 62 pp.

Cimorelli, A.J., Perry, S.G., Venkatram, A., Weil, J.C., Paine, R.J., Wilson, R.B., Lee, R.F., Peters, W.D., Brode, R.W., and Paumier, J.O., 2004: *AERMOD: Description of model formulation*. U.S. Environmental Protection Agency, report-454/R-03-004, 91 pp.

Clarke, M.C.G., Woodhall, D.G., Allen, D., and Darling, G., 1990: *Geological, volcanological and hydrogeological controls of the occurrence of geothermal activity in the area surrounding Lake Naivasha, Kenya*. Ministry of Energy, Nairobi, 138 pp.

Ermak, D.L, Nyholm, R.A., and Gudilsen, P.H., 1980: Potential air quality impacts of large-scale geothermal energy development in the Imperial Valley, California, USA. *Atmos. Environ., 14*, 1321-1330.

Gallegos-Ortega, R., Quintero-Nuñez, M., and García-Cueto, O., 2000: H_2S dispersion model at Cerro Prieto geothermoelectric power plant. *Proceedings of the World Geothermal Congress 2000*, *Kyushu-Tohoku, Japan,* 579-584.

Giroud, N., and Arnórsson, S., 2005: Estimation of long-term CO_2 and H_2S release during operation of geothermal power plants. *Proceedings of the World Geothermal Congress* 2005, Antalya, Turkey, 6 pp.

Haralabidis, A.S., Dimakopoulou, K., Vigna-Taglianti, F., Giampaolo, M., Borgini, A., and Dudley, M.L., 2008: Acute effects of night-time noise exposure on blood pressure in populations living near airports. *European Heart Journal, 29*, *658*-664.

Holmes Air Sciences, 2009: *Olkaria II geothermal power plant project hydrogen sulphide dispersion study of the effects of emissions from unit 3. Air quality impact assessment report*. Mitsubishi Heavy Industries, Ltd., Japan, Holmes Air Sciences, Australia, 41 pp.

Hunt, T.M., 2001: *Five lectures on environmental effects of geothermal utilization.* UNU-GTP, Iceland, report 1-2000, 109 pp.

Ismail, A.R., Nor, M.J.M., Mansor, M.R.A., Tahir, M.F.M., and Zulkifli, R., 2009: Environmental noise assessment and modelling in Malaysia: A comparative monitoring study. *European J. Scientific Research 30-2,* 236-244.

Karekezi, S., and Kithyoma, W., 2003: Renewable energy development. *Workshop for African Energy Experts on Operationalizing the NEPAD Energy Initiative, Dakar, Senegal,* 27 pp.

KNBS, 2009: *Population and housing census for 2009*. Kenya National Bureau of Statistics, website: *www.knbs.or.ke*.

Kollikho P., and Kubo, B., 2001: Olkaria geothermal power plant gaseous emissions – A flower trial case study. *Geoth. Res. Council, Transactions, 25,* 257-261.

Komurcu, M.I., and Akpinar, A., 2009: Importance of geothermal energy and its environmental effects in Turkey. *Renewable Energy, 34*, 1611-1615.

Kristmannsdóttir, H., Sigurgeirsson, M., Ármannsson, H., Hjartarsson, H., and Ólafsson, M., 2000: Sulphur gas emissions from geothermal power plants in Iceland. *Geothermics, 29*, 525-538.

Lagat, J.K., 2004: *Geology, hydrothermal alteration and fluid inclusion studies of Olkaria Domes geothermal field, Kenya.* University of Iceland, Msc Thesis, UNU-GTP, Iceland, report 1, 71 pp.

Lund, J.W., Freeston, D.H., and Boyd, T.L., 2010: Direct utilization of geothermal energy 2010 worldwide review. *Proceedings of the World Geothermal Congress 2010, Bali, Indonesia*, 23 pp.

Macdonald, R., 2003: *Theory and objectives of air dispersion modelling*. The University of Western Ontario, Faculty of Engineering, 27 pp., website: *www.engga.uwo.ca/people/esavory/MME474A_Part1.pdf.*

Marani, M., Tole, M., and Ogalo, L., 2000: Concentrations of hydrogen sulphide in air around the Olkaria geothermal field, Kenya. *Proceedings of the World Geothermal Congress 2000*, *Kyushu-Tohoku, Japan,* 649-661.

Marouli, C., and Kaldellis, J.K., 2001: Risk in the Greek electricity production sector. *Proceedings of the 7th International Conference on Environmental Science and Technology, Ermoupolis, Syros Island, Greece,* 305–314.

Muzet, A., 2007: Environmental noise, sleep and health. *Sleep Medicine Reviews, 11,* 135-142.

Nyagah, E.M., 2006: Hydrogen sulphide dispersion and modelling for Nesjavellir power station using Gaussian and numerical models. Report 15 in: *Geothermal Training in Iceland 2006.* UNU-GTP, Iceland, 291-314.

Opondo, K.M., 2007: *Corrosive species and scaling in wells at Olkaria, Kenya and Reykjanes, Svartsengi and Nesjavellir, Iceland.* University of Iceland, MSc thesis, UNU-GTP, Iceland, report 2, 76 pp.

Republic of Kenya, 2009: *Environment management and co-ordination (noise and excessive vibration pollution control) regulations, 2009*. Government of Kenya, Legal notice no. 61, Government printer, Nairobi, 23 pp.

Republic of Kenya, 2010: *Least cost power development plan, study period 2010-2030*. Ministry of Energy, Kenya, 147 pp.

Rybach, L., 2003: Geothermal energy: sustainability and the environment. *Geothermics, 32,* 463-470.

Seinfeld, J.H., and Pandis, S.N., 2006: Atmospheric diffusion. In: *Atmospheric chemistry and physics, from air pollution to climate change (*2nd ed.), John Wiley and Sons, Inc. 828-899.

Simiyu, S.M., 2008: Kenya's geothermal expansion strategy for developing 1260 MWe by 2018. *Geoth. Res. Council, Transactions, 32*, 369-372.

Simiyu, S.M., 2010: Status of geothermal exploration in Kenya and future plans for its development. *Proceedings of the World Geothermal Congress 2010, Bali, Indonesia*, 11 pp.

Sinclair Knight and Partners, 1994: *Environmental assessment for north east Olkaria power development project*. Report for the KenGen Company Ltd., RSP International Ltd., 800 pp.

Webster, J.G., 1995: Chemical impacts of geothermal development. In: Brown, K.L. (convenor), *Environmental aspects of geothermal development*. World Geothermal Congress 1995, IGA pre-congress course, Pisa, Italy, 79-95.

Were, J.O., 2007: *The speciation of trace elements in spent geothermal fluids and implications for environmental health around Olkaria, Kenya.* University of Iceland, MSc Thesis, UNU-GTP, Iceland, report 1, 73 pp.

WHO, 1981: *Hydrogen sulphide.* World Health Organization, Geneva, Environmental health criteria, no. 19.

WHO, 1999: *Guidelines for community noise*. World Health Organization, Geneva, 141 pp.

WHO, 2000: *Air quality guidelines for Europe* (2nd ed.). WHO regional publications, European Series no. 91, 273 pp.

WHO, 2003: *Hydrogen sulphide: human health aspects*. World Health Organization, Geneva, Concise international chemical assessment document 53, 35 pp., website: *www.who.int/ipcs/publications/cicad/en/cicad53.pdf.*

World Bank, 1998: *Pollution prevention and abatement handbook. Toward cleaner production*, World Bank Group, Washington, DC, 471 pp.

World Bank, 2007: *Environmental, health and safety (EHS) guidelines*, World Bank Group, Washington, DC, 99 pp.